Microbial superoxide production drives biogenic nitrogen dioxide formation in soils

Megan L. Purchase[a], Jonathan D. Raff[b], Deying Wang[a], and Ryan M. Mushinski[a,*]

Author affiliations:

[a]School of Life Sciences, University of Warwick, Coventry CV4 7AL, United Kingdom

[b]Paul H. O'Neill School of Public and Environmental Affairs, Indiana University, Bloomington, IN 47405, USA

*Corresponding author. Email: Ryan.Mushinski@warwick.ac.uk

Nitrogen dioxide (NO_2) is a critical atmospheric pollutant and ozone precursor, yet biogenic soil sources remain poorly constrained. Current models assume soil NO_2 flux is exclusively depositional. Here we demonstrate that soils can produce NO_2 through microbial superoxide (O_2^-) production. Using manipulative slurry experiments, native microbial communities produced 6-10 times more NO_2 than sterile controls following nitric oxide (NO) exposure. Stimulating superoxide production with NADH increased NO_2 formation 15-fold, while inhibiting NADH oxidase reduced production to near-sterile levels. Superoxide dismutase decreased NO_2 production by 50-75%, and O_2^- concentration explained 60% of variation in NO_2 production rates. Addition of peroxynitrite to soil increased headspace NO_2, confirming this intermediate as the mechanistic link. These findings reveal a novel pathway linking carbon and nitrogen cycling where heterotrophic decomposers facilitate biogenic NO-to-NO_2 conversion via superoxide chemistry, potentially explaining discrepancies between satellite observations and modelled soil NO_x emissions.

soil biogeochemistry | superoxide | peroxynitrite | nitrogen dioxide

Soils contribute approximately 15% of the global land-to-atmosphere NOx flux, estimated at 9-10 Tg N y^{-1} (1). Current biogeochemical models treat these emissions as exclusively nitric oxide (NO), assuming any NO_2 in the soil-atmosphere exchange results entirely from atmospheric oxidation of emitted NO or from deposition. However, satellite observations consistently reveal discrepancies with bottom-up model estimates. Pre-2012 models underestimated observed NO_2 columns by factors of 2-4 over North America and Africa, and recent studies suggest natural NO_x from Amazonian and agricultural soils may be 10–20 times larger than current model inventories (2-4). These persistent discrepancies suggest undefined pathways for gaseous NO_x production from soil, potentially including direct biogenic NO_2 formation.

Recent advances in understanding microbial reactive oxygen species production offer a potential mechanism for biogenic NO_2 formation. Heterotrophic bacteria and fungi produce extracellular superoxide (O_2^-) through the activity of NADH oxidases and other oxidoreductases (5). In physiological systems, O_2^- reacts rapidly with NO at near diffusion-limited rates ($k > 10^9$ M^{-1} s^{-1}) to form peroxynitrite ($ONOO^-$), which subsequently decomposes to yield NO_2 and other reactive nitrogen species (6). We hypothesised that this well-characterised physiological chemistry could occur in soils where nitrogen-cycling microorganisms produce NO through nitrification and denitrification while heterotrophic decomposers produce superoxide.

Using manipulative slurry experiments with agricultural (sandy loam, pH 6.8, 3.2% organic matter) and woodland (clay loam, pH 5.9, 8.1% organic matter) soils from Warwickshire, UK, we tested this mechanism through selective stimulation and inhibition of superoxide-producing pathways. Sterile soil showed minimal NO_2 accumulation following NO addition (agricultural: 0.72 ± 0.53 ppb h^{-1}; woodland: 1.10 ± 0.74 ppb h^{-1}), representing baseline abiotic conversion. In contrast, native soils with intact microbial communities produced significantly elevated NO_2, with 10-fold higher concentrations in agricultural soil (7.42 ± 2.61 ppb h^{-1}; $p < 0.001$) and 6-fold higher in woodland soil (6.90 ± 4.37 ppb h^{-1}; $p < 0.001$; **Fig. 1A**). This demonstrates that soil microorganisms actively convert NO to NO_2 under aerobic conditions.

NADH addition to stimulate extracellular superoxide production via NADH oxidase activity dramatically increased NO_2 formation, with 15-fold increase relative to sterile controls in agricultural soil (10.90 ± 8.21 ppb h^{-1}) and 16-fold increase in woodland soil (18.02 ± 8.00 ppb h^{-1}; $p < 0.001$). When diphenyleneiodonium (DPI) was co-applied to inhibit flavin-containing NADH oxidases, NO_2 production was reduced to levels not significantly different from sterile controls ($p > 0.05$), indicating that NADH oxidase activity is necessary for biogenic NO_2 production. Concurrent measurement of extracellular superoxide revealed a strong positive correlation with NO_2 production across all treatments and soil types ($r = 0.77$, $R^2 = 0.60$, $p < 0.001$; **Fig. 1B**), supporting the proposed mechanism. The conversion efficiency of NO-to-NO_2 was approximately 63% in biotic treatments (**Fig. 1C**), and production rates increased strongly with temperature (**Fig. 1D**), consistent with enzymatic processes.

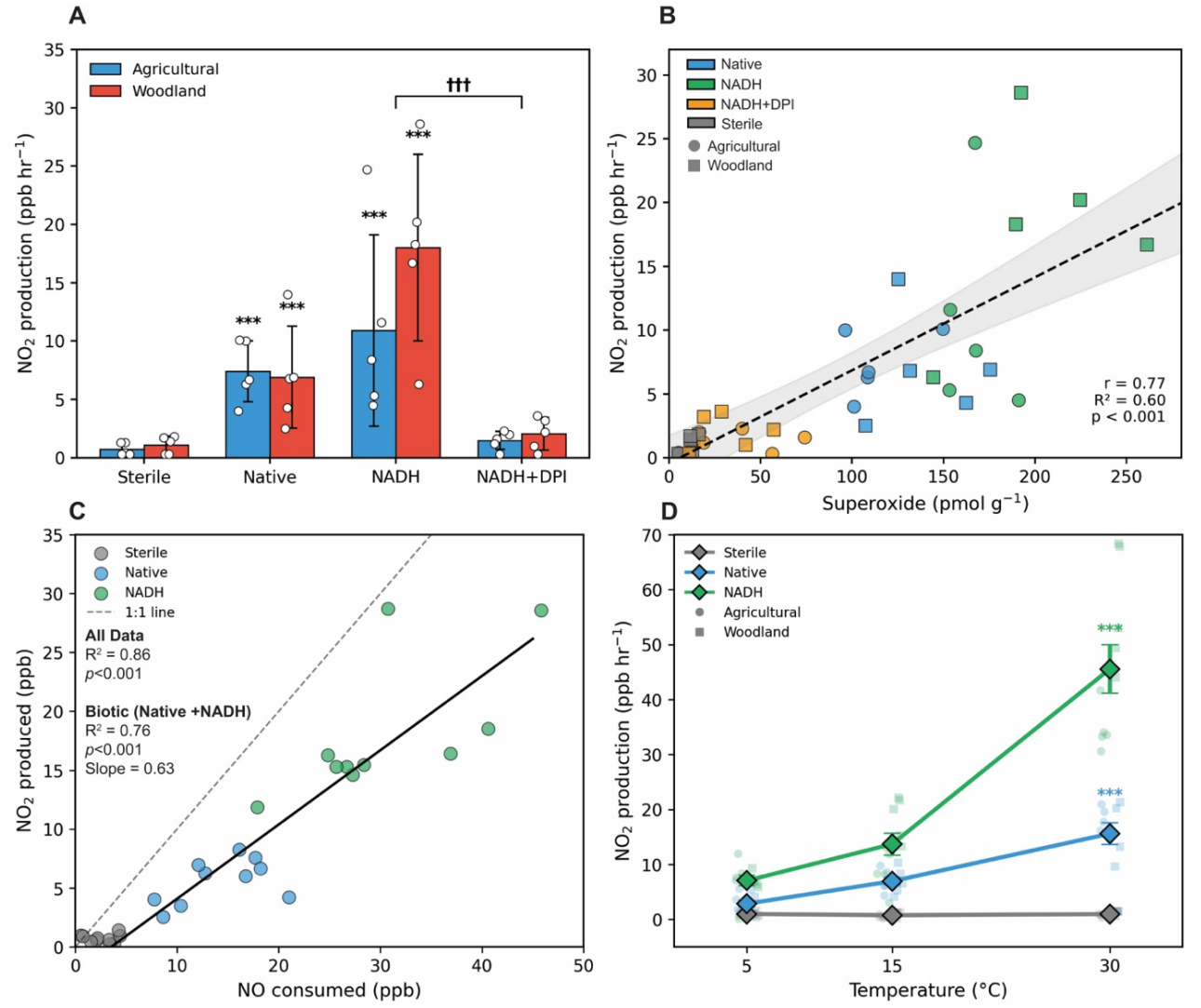

Fig. 1. Biogenic NO_2 production from soil microbial activity. (A) NO_2 production rates across treatments in agricultural (blue) and woodland (red) soils. Data are mean ± SE with individual replicates shown; ***p < 0.001 vs. sterile, $^{\dagger\dagger\dagger}p$ < 0.001 NADH vs. NADH+DPI. (B) Correlation between superoxide production and NO_2 emission rates across treatments (r = 0.77, R^2 = 0.60, p < 0.001). Circles = agricultural; squares = woodland. (C) Relationship between NO consumed and NO_2 produced showing 63% conversion efficiency in biotic treatments. (D) Temperature dependence of NO_2 production (***p< 0.001 vs. 5°C).

To directly test whether superoxide is required for NO_2 formation rather than simply correlated, we added superoxide dismutase (SOD) to convert O_2^- to hydrogen peroxide (H_2O_2) before it could react with NO. SOD addition reduced NO_2 production in live treatments but had minimal effect on sterile controls. In woodland soil, where baseline production was highest, SOD reduced NO_2 production by 75% in native treatments (from 16.7 ± 6.7 to 4.6 ± 2.5 ppb h^{-1}; p < 0.01) and by 50% in NADH treatments (p < 0.05; **Fig. 2A**). Importantly, heat-inactivated SOD (boiled 10 min) had no significant effect on NO_2 production (p > 0.05; **Fig. 2B**), confirming that the observed reduction is due to enzymatic superoxide scavenging rather than non-specific protein effects.

If the proposed mechanism is correct, that superoxide reacts with NO to form peroxynitrite, which then decomposes to NO_2, then direct addition of peroxynitrite to soil should enhance NO_2 emissions. Addition of synthesised $ONOO^-$ (0.08–0.32 μM) to soil microcosms significantly increased NO_2 + NO_z [NO_z = Total Reactive N-oxides – NO_x] fluxes compared to water controls ($p < 0.001$ for all concentrations vs. baseline; **Fig. 2C**). Additional soil validation experiments confirmed that peroxynitrite addition significantly increased both NO_2 and NO_z concentrations across agricultural and woodland soils (**Fig. 2D**). This confirms that peroxynitrite decomposition in soil produces NO_2 that can be emitted past the soil-atmosphere interface.

As depicted in **Fig. 2E**, the proposed mechanism proceeds through the reaction, $NO + O_2^- \rightarrow ONOO^-$, followed by peroxynitrite decomposition to yield NO_2 and hydroxyl radical (7). This pathway would be most significant in soils with active nitrogen cycling producing NO and high heterotrophic activity from organic matter decomposition producing superoxide, conditions possibly incurred in fertilised agricultural soils following nitrogen application and in organic-rich forest ecosystems. The approximately 25–50% residual NO_2 production after SOD addition may indicate incomplete O_2^- scavenging in the soil matrix or contributions from hydroperoxyl radical (HO_2•), which predominates below pH 4.8 and reacts with SOD at rates several orders of magnitude lower than O_2^- (8). Given our bulk soil pH values of 5.9–6.8, HO_2• would represent a minor fraction under bulk conditions.

These findings have important implications for understanding previous measurements of soil NO_x budgets and the persistent discrepancies between satellite observations and bottom-up models. Current biogeochemical models do not include this pathway, potentially leading to systematic underestimation of soil NO_x emissions. Our results extend previous observations that some forest soils emit NO_2 rather than acting exclusively as sinks (9), providing a mechanistic framework explaining why emission versus deposition depends on soil biogeochemical conditions. Soils with high organic matter, supporting heterotrophic superoxide production, combined with active nitrogen cycling would favour NO_2 production and potential emission. Soil emissions of NO_2 have been previously reported; for example, Williams et al. using chambers in the field estimated that NO_2 fluxes were 10% those of NO (10). However, the origin of the emissions was not clear at the time. This work also implies that some of the $HONO_{(g)}$ soil emissions reported could stem from NO_2-to-HONO conversion on soil surfaces as previously described (11, 12). Thus, it is possible that NO_2 formation in soil has been underreported due its rapid conversion into HONO on soil surfaces. The discovery that heterotrophic activity directly influences reactive nitrogen emissions represents a previously unrecognised link between terrestrial carbon and nitrogen cycling that should be incorporated into Earth system models.

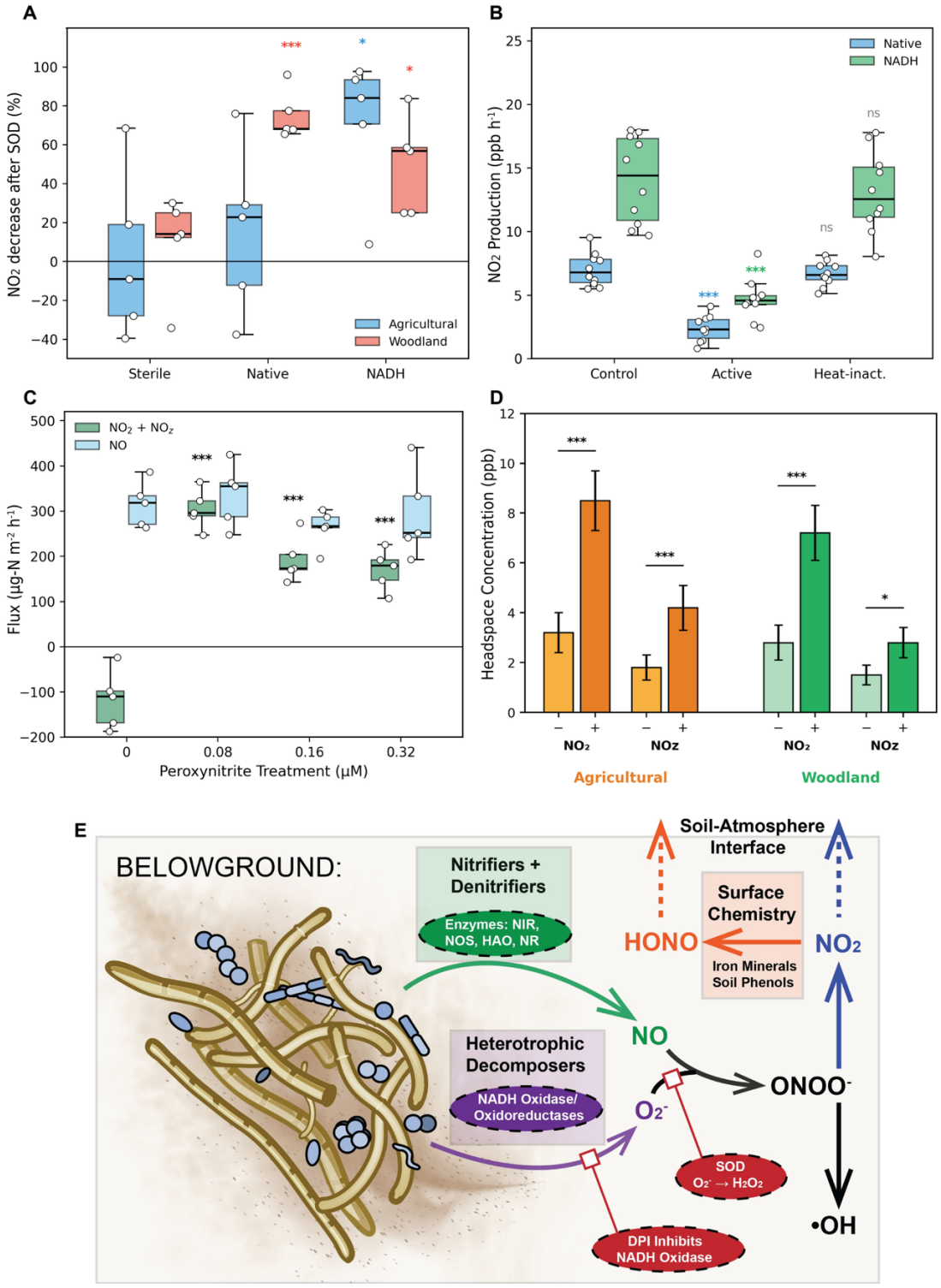

Fig. 2. Superoxide and peroxynitrite mediate NO_2 formation. (A) Percent NO_2 decrease after SOD addition. (B) Active vs. heat-inactivated SOD control of NO_2 production; ***p < 0.001, ns = not significant. (C) NO_2 flux response to peroxynitrite dose (***p < 0.001 vs. baseline). (D) Additional soil validation with ±$ONOO^-$ treatments. (E) Proposed mechanism for biogenic NO_2 production from soils. Nitrifiers and denitrifiers produce nitric oxide (NO) via key nitrogen-cycling enzymes (NIR, NOS, HAO, NR). Heterotrophic decomposers generate extracellular superoxide (O_2^-) through NADH oxidase and oxidoreductases. NO and O_2^- react to form peroxynitrite ($ONOO^-$), which decomposes to NO_2 and hydroxyl radical (•OH). NO_2 is emitted across the soil-atmosphere interface or converted to HONO via surface chemistry involving iron minerals and soil phenols. Red inhibitors show experimental controls of the superoxide mechanism, where diphenyleneiodonium (DPI) blocks NADH oxidase; superoxide dismutase (SOD) scavenges O_2^-, confirming superoxide-dependent NO_2 formation.

Materials and Methods

Soils were collected from agricultural (winter wheat) and woodland sites at the University of Warwick's Stratford Innovation Campus. Samples were sieved (2 mm), adjusted to 60% water holding capacity, and pre-incubated at 25°C for 7 days. Sterile controls were prepared by autoclave sterilisation. Aerobic slurries (100 g soil, 60 mL water) received four treatments (n = 5): sterile, native, NADH-amended (0.3 μmol g^{-1}), or NADH+DPI (10 μM). Following 45 ppb NO addition, headspace NO_2 was monitored continuously for 120 min using an ICAD-HONO/NO_2 200L analyser (AirYX GmbH) employing cavity-enhanced differential optical absorption spectroscopy (detection limit: 0.4 ppb). Extracellular superoxide was quantified via hydroethidine oxidation and cytochrome c reduction (13, 14). For SOD experiments, 500 U ml^{-1} active or heat-inactivated (100°C, 10 min) SOD was added. Peroxynitrite was synthesised from acidified H_2O_2 and $NaNO_2$ (15). Data were analysed using one-way ANOVA with Tukey's HSD and paired t-tests (α = 0.05). Detailed methodology can be found in the supplemental information.

Data, Materials, and Software Availability

All study data are included in the article and/or supporting information.

ACKNOWLEDGMENTS

Financial support was provided by UKRI NERC (CENTA2; NE/S007350/1) and UKRI BBSRC (BB/X002187/1). JDR's contribution was supported by the U.S. National Science Foundation (Award #2243202).

References

1. H. Weng *et al.*, Global high-resolution emissions of soil NO_x, sea salt aerosols, and biogenic volatile organic compounds. *Scientific Data* **7**, 148 (2020).

2. R. C. Hudman *et al.*, Steps towards a mechanistic model of global soil nitric oxide emissions: implementation and space based-constraints. *Atmos. Chem. Phys.* **12**, 7779-7795 (2012).

3. B. H. Lee *et al.*, Sensitive Response of Atmospheric Oxidative Capacity to the Uncertainty in the Emissions of Nitric Oxide (NO) From Soils in Amazonia. *Geophysical Research Letters* **51**, e2023GL107214 (2024).

4. B. Opacka *et al.*, Natural emissions of VOC and NO_x over Africa constrained by TROPOMI HCHO and NO_2 data using the MAGRITTEv1.1 model. *Atmos. Chem. Phys.* **25**, 2863-2894 (2025).

5. J. M. Diaz *et al.*, Widespread Production of Extracellular Superoxide by Heterotrophic Bacteria. *Science* **340**, 1223-1226 (2013).

6. G. Merényi, J. Lind, S. Goldstein, G. Czapski, Mechanism and Thermochemistry of Peroxynitrite Decomposition in Water. *The Journal of Physical Chemistry A* **103**, 5685-5691 (1999).

7. R. E. Huie, S. Padmaja, The Reaction of NO With Superoxide. *Free Radical Research Communications* **18**, 195-199 (1993).

8. B. H. J. Bielski, D. E. Cabelli, R. L. Arudi, A. B. Ross, Reactivity of HO_2/O^-_2 Radicals in Aqueous Solution. *Journal of Physical and Chemical Reference Data* **14**, 1041-1100 (1985).

9. R. M. Mushinski *et al.*, Microbial mechanisms and ecosystem flux estimation for aerobic NOy emissions from deciduous forest soils. *Proceedings of the National Academy of Sciences* 10.1073/pnas.1814632116, 201814632 (2019).

10. E. J. Williams, D. D. Parrish, F. C. Fehsenfeld, Determination of nitrogen oxide emissions from soils: Results from a grassland site in Colorado, United States. *Journal of Geophysical Research: Atmospheres* **92**, 2173-2179 (1987).

11. M. A. Kebede, D. L. Bish, Y. Losovyj, M. H. Engelhard, J. D. Raff, The Role of Iron-Bearing Minerals in NO_2 to HONO Conversion on Soil Surfaces. *Environmental Science & Technology* **50**, 8649-8660 (2016).

12. N. K. Scharko, E. T. Martin, Y. Losovyj, D. G. Peters, J. D. Raff, Evidence for Quinone Redox Chemistry Mediating Daytime and Nighttime NO_2-to-HONO Conversion on Soil Surfaces. *Environmental Science & Technology* **51**, 9633-9643 (2017).

13. J. M. Diaz *et al.*, NADPH-dependent extracellular superoxide production is vital to photophysiology in the marine diatom *Thalassiosira oceanica*. *Proceedings of the National Academy of Sciences* **116**, 16448-16453 (2019).

14. C. D. Georgiou, I. Papapostolou, K. Grintzalis, Superoxide radical detection in cells, tissues, organisms (animals, plants, insects, microorganisms) and soils. *Nature Protocols* **3**, 1679-1692 (2008).

15. K. M. Robinson, J. S. Beckman, "Synthesis of Peroxynitrite from Nitrite and Hydrogen Peroxide" in Methods in Enzymology. (Academic Press, 2005), vol. 396, pp. 207-214.

Supporting Information for

Microbial superoxide production drives biogenic nitrogen dioxide formation in soils

Megan L. Purchase, Jonathan D. Raff, Deying Wang, and Ryan M. Mushinski*
*Corresponding Author's Email: Ryan.Mushinski@warwick.ac.uk

This PDF file includes:

Supporting Materials and Methods

Supporting Materials and Methods

1. Soil Collection and Characterisation

Soils were collected in September 2024 from two contrasting land-use types at the University of Warwick's Stratford Innovation Campus (52.205°N, 1.602°W). The agricultural site was under continuous winter wheat cultivation (cv. Skyfall) with conventional tillage and fertilisation practices (120 kg N ha^{-1} y^{-1} as urea). The woodland site was a mature mixed deciduous woodland dominated by *Quercus robur* and *Fraxinus excelsior* with no management intervention for >30 years.

At each site, five replicate sampling points were established along a 30 m transect with 5 m spacing. At each point, surface litter was removed and soil cores (5 cm diameter x 15 cm depth) were collected using sterile PVC corers. Cores were immediately placed in sterile polyethylene bags, stored on ice, and transported to the laboratory within 2 hours of collection. Soils were homogenised by passing through a 2 mm stainless steel sieve. Sieved soils were stored at 4°C until use.

Soil physicochemical properties were determined using standard methods. Soil texture was analysed using the hydrometer method. Soil pH was measured in a 1:2 (w/v) soil:deionised water suspension using a calibrated glass electrode (Mettler Toledo). Organic matter content was determined by loss-on-ignition at 550°C for 4 hours. Total carbon and nitrogen were quantified by dry combustion (Elementar vario PYRO cube). Gravimetric water content was determined by oven-drying at 100°C for 24 hours, and water holding capacity (WHC) was measured using the funnel method with 24-hour drainage.

The agricultural soil was a sandy loam (60 ± 3% sand, 25 ± 2% silt, 15 ± 2% clay), while the woodland soil was a clay loam (32 ± 4% sand, 35 ± 3% silt, 33 ± 4% clay). Soil pH was 6.8 ± 0.3 in the agricultural soil and 5.9 ± 0.2 in the woodland soil. Organic matter content was 3.2 ± 0.4% and 8.1 ± 0.6% in the agricultural and woodland soils, respectively. Total C was 18.6 ± 2.1 g kg^{-1} (agricultural) and 47.2 ± 3.8 g kg^{-1} (woodland), and total N was 1.9 ± 0.2 g kg^{-1} and 4.1 ± 0.4 g kg^{-1}, respectively. C:N ratios were 9.8 ± 0.5 and 11.5 ± 0.8, and water holding capacity was 0.42 ± 0.03 g g^{-1} and 0.68 ± 0.05 g g^{-1}, for the agricultural and woodland soils, respectively. All values are mean ± SD (n = 5).

2. Soil Sterilisation

Sterile controls were prepared by autoclaving following validated protocols (1). Fresh sieved soil (100 g) was placed in autoclavable polypropylene containers with loosened lids and autoclaved at 121°C and 103 kPa (15 psi) for 30 minutes. Soils were allowed to cool to room temperature, mixed thoroughly, and the process repeated twice more at 24-hour intervals to eliminate heat-resistant endospores that may germinate between cycles. Sterilisation efficacy was verified by absence of CO_2 evolution over 7 days at 25°C and no colony formation on tryptic soy agar plates inoculated with soil suspensions. Sterile soils were stored at 4°C and used within 24 hours of the final autoclave cycle.

3. Slurry Incubation Experiments

Aerobic soil slurries were prepared by combining soil (100 g dry weight equivalent) with sterile deionised water (60 ml) in 250 ml borosilicate glass bottles (Wheaton) fitted with butyl rubber septa. The soil:water ratio (1:0.6 w/v) was selected to maintain aerobic conditions while ensuring adequate mixing and reagent diffusion. Slurries were pre-incubated at 25°C with orbital shaking (150 rpm) for 24 hours to equilibrate microbial activity before experimental treatments. Gas diffusion was maintained during pre-incubation with a 23-gauge needle in the butyl stopper.

Four experimental treatments were applied (n = 5 biological replicates per treatment per soil type): (i) Sterilised soil with no amendments (sterile); (ii) Untreated soil with intact microbial communities (Native); (iii) Native soil amended with reduced β-nicotinamide adenine dinucleotide (NADH; 0.3 μmol g^{-1} soil; Sigma-Aldrich, ≥97% purity); (iv) Native soil amended with NADH (0.3 μmol g^{-1}) plus diphenyleneiodonium chloride (NADH+DPI; 10 μM final concentration; Sigma-Aldrich, ≥98% purity).

NADH was dissolved in sterile deionised water immediately before use and added to slurries via syringe injection through the septum. DPI was dissolved in dimethyl sulfoxide (DMSO; final DMSO

concentration <0.1% v/v) and pre-incubated with slurries for 30 minutes before NADH addition to allow enzyme inhibition. Control treatments received equivalent volumes of vehicle (water or DMSO).

The NADH concentration (0.3 μmol g^{-1}) was selected based on preliminary dose-response experiments showing maximal superoxide stimulation without substrate inhibition. DPI concentration (10 μM) was chosen to achieve >90% inhibition of flavin-containing NADH oxidases based on published K_i values (2).

4. Nitric Oxide Exposure and Nitrogen Dioxide Quantification

Following treatment application, slurry headspace was flushed with synthetic air (79% N_2, 21% O_2; BOC) for 5 minutes to establish baseline conditions. Baseline headspace NO_2 concentration was measured, then nitric oxide (45 ppb in N_2) was introduced by replacing 50 ml of headspace with calibrated NO gas mixture via gas-tight syringe. The 45 ppb NO concentration was selected to represent the upper range of soil pore-space NO concentrations observed in agricultural soils following fertilisation. It is important to note that the synthetic air carrier gas used was free of ozone, which precludes NO-to-NO_2 conversion via NO + O_3 reaction from impacting our results (3).

Headspace NO_2 accumulation was monitored before NO addition, directly after, at 60 min, and at 120 minutes using an AIRYX ICAD-HONO/NO_2-200L analyser (Airyx GmbH, Germany). Measurement vessels were covered in aluminium foil during the experiment to exclude unintended photolytic effects. NO_2 production rates were calculated as the slope of linear regression of headspace concentration versus time, expressed as ppb hr^{-1}. The instrument employs incoherent broadband cavity-enhanced absorption spectroscopy (IBBCEAS) with iterative spectral fitting, providing direct (absolute) NO_2 measurement without chemical conversion or interference from other nitrogen oxides (4). The optical path length was 2.4 km (effective), achieved through ~4,800 reflections in a 0.5 m cavity with mirrors of 99.99% reflectivity. Spectra were acquired at 1 Hz and averaged to 10-second intervals for analysis.

5. Extracellular Superoxide Quantification

Extracellular superoxide (O_2^-) was quantified using a dual-assay approach combining hydroethidine (HE) oxidation and ferricytochrome c reduction, following established protocols for soil systems (5). Soil extracts were prepared by adding 10 ml ice-cold phosphate buffer (50 mM, pH 7.4, supplemented with 100 μM diethylenetriaminepentaacetic acid [DTPA] to chelate transition metals) to 5 g soil, from the 120 min timepoint samples. Suspensions were vortexed for 2 minutes, centrifuged at 5,000 x g for 10 minutes at 4°C, and supernatants filtered through 0.45 μm cellulose acetate filters (Whatman). Extracts were analysed immediately to minimise superoxide decay.

5.1 Hydroethidine assay

Soil extract (100 μL) was combined with hydroethidine (10 μL of 10 mM stock in DMSO; final concentration 1 mM; ABCR UK LTD, ≥95% purity) in black 96-well microplates. Parallel wells received superoxide dismutase (SOD; 500 U ml^{-1}; Sigma Aldrich, ≥95 % by biuret) to distinguish superoxide-specific oxidation from non-specific fluorescence. Plates were incubated for 15 minutes at 25°C in darkness, and fluorescence of the superoxide-specific product 2-hydroxyethidium (2-OH-E^+) was measured at λex = 480 nm, λem = 580 nm using a FLUOstar Omega (BMG Labtech) microplate reader (6).

5.2 Cytochrome c assay

Soil extract (200 μL) was added to ferricytochrome c (50 μM final concentration; from bovine heart, Sigma-Aldrich, ≥95% based on molecular weight) in clear 96-well plates. Reduction of cytochrome c was monitored at 550 nm for 10 minutes. The SOD-inhibitable fraction was determined by parallel incubations with 500 U ml^{-1} SOD. Superoxide concentration was calculated using $\Delta\varepsilon_{550}$ = 21.1 mM^{-1} cm^{-1}. Standard curves were prepared using superoxide generated by the xanthine (50 μM) / xanthine oxidase (0.01 U ml^{-1}) system, with superoxide concentrations calculated from the rate of cytochrome c

reduction. Results from both assays were averaged and expressed as pmol O_2^- g^{-1} dry soil. The detection limit was 11 pmol g^{-1} (3σ of blank).

6. Superoxide Dismutase Scavenging Experiments

To directly test the requirement for superoxide in NO_2 formation, exogenous superoxide dismutase (SOD) was added to scavenge O_2^- before it could react with NO. SOD from bovine erythrocytes (Sigma-Aldrich, ≥3,000 U mg^{-1} protein) was dissolved in phosphate buffer (50 mM, pH 7.4) and added to slurries at a final concentration of 500 U ml^{-1}. This concentration was selected to achieve complete superoxide scavenging based on the measured superoxide production rates and SOD kinetics (k_{cat} = 2 × 10^9 M^{-1} s^{-1}).

Heat-inactivated SOD controls were prepared by incubating SOD solution (1,000 U ml^{-1}) at 100°C for 10 minutes, which eliminates enzymatic activity. Complete inactivation was verified by cytochrome c reduction assay. Comparison of active versus heat-inactivated SOD effects distinguished enzymatic superoxide scavenging from potential non-specific effects of protein addition (e.g., NO binding, surface interactions). SOD was added to slurries 5 minutes before NO introduction. NO_2 production rates were measured as described above, and the SOD-sensitive fraction was calculated as,

$$NO2_{SOD} = \frac{Rate\ without\ SOD - Rate\ with\ SOD}{Rate\ without\ SOD} \times 100$$

7. Peroxynitrite Synthesis and Addition Experiments

Peroxynitrite ($ONOO^-$) was synthesised by the reaction of acidified hydrogen peroxide with sodium nitrite, following established methods (7). Briefly, ice-cold solutions of $NaNO_2$ (0.6 M) and H_2O_2 (0.6 M in 0.7 M HCl) were mixed rapidly using a quenched-flow reactor, and the product immediately quenched with excess NaOH (1.5 M) to yield alkaline peroxynitrite stock (~180 mM). Concentration was determined spectrophotometrically at 302 nm. Stocks were stored at -80°C in small aliquots and used within 2 weeks. Purity was verified by the absence of significant absorbance at 350 nm (indicating minimal nitrite contamination).

For dose-response experiments, sterile soil (200 g) was placed in fluropolymer-coated PVC microcosms (~0.6 L) with continuous headspace monitoring. Peroxynitrite was diluted in ice-cold NaOH (10 mM) immediately before use and applied to the soil surface at concentrations of 0 (NaOH vehicle), 0.08, 0.16, and 0.32 µM (per gram soil). Headspace total reactive nitrogen oxides (NOz = NOy − NOx) were monitored for 60 minutes using a Teledyne T200U-NOy chemiluminescence analyser. The T200U employs molybdenum catalytic conversion at 325°C for NOy measurement and direct chemiluminescence for NO.

For field-fresh soil validation experiments, soil slurries (5 g soil in 15 ml deionised water) in 50 ml serum vials were amended with either 0.01 µM $ONOO^-$ or vehicle (NaOH) and incubated at 25°C with orbital shaking (150 rpm) for 8 hours. Headspace was sampled at t = 0, 2, 4, 6, and 8 hours and analysed for NO, NO_2, and NOz by chemiluminescence.

8. Temperature Response Experiments

To assess the temperature dependence of biogenic NO_2 production, slurry incubations were conducted at 5°C, 15°C, and 30°C in temperature-controlled incubators (±0.5°C). Slurries were equilibrated at the target temperature for 2 hours before NO addition and measurements.

9. Nitric Oxide Consumption and Conversion Efficiency

To quantify the stoichiometry of NO-to-NO_2 conversion, headspace NO was monitored simultaneously with NO_2. NO consumption was calculated as the decrease in headspace NO concentration over 60 minutes. Conversion efficiency was calculated as,

$$CE_{NO \rightarrow NO2} = \left(\frac{NO2\ produced}{NO\ consumed}\right) \times 100$$

The theoretical maximum for the superoxide mechanism is 100% (e.g., 1 NO + 1 O_2^- → 1 $ONOO^-$→ 1 NO_2), though competing reactions reduce observed efficiency. As noted above, NO-to-NO_2 conversion is not due to NO oxidation by ozone, since its concentration is negligible under the conditions of our experiments.

10. Statistical Analysis

All statistical analyses were performed in R (version 4.3.0; R Core Team, 2023). Data were tested for normality (Shapiro-Wilk test) and homogeneity of variance (Levene's test) before parametric analyses. Treatment effects on NO_2 production rates were assessed using one-way analysis of variance (ANOVA) with Tukey's Honest Significant Difference (HSD) post-hoc tests for multiple comparisons. Effects of SOD addition were analysed using paired t-tests comparing rates before and after SOD treatment. Correlations between superoxide concentration and NO_2 production were assessed using Pearson's product-moment correlation coefficient. Temperature effects were analysed using two-way ANOVA with temperature and treatment as factors. Statistical significance was set at $\alpha = 0.05$. Effect sizes were calculated as Cohen's d for pairwise comparisons. All reported uncertainties are standard deviations (SD) unless otherwise specified. Figures show individual data points overlaid on summary statistics (mean ± SD or mean ± SEM as indicated) to display data distribution.

Supporting References

1. D. C. Wolf, T. H. Dao, H. D. Scott, T. L. Lavy, Influence of Sterilization Methods on Selected Soil Microbiological, Physical, and Chemical Properties. *Journal of Environmental Quality* **18**, 39-44 (1989).
2. V. B. O'Donnell, D. G. Tew, O. T. G. Jones, P. J. England, Studies on the inhibitory mechanism of iodonium compounds with special reference to neutrophil NADPH oxidase. *Biochemical Journal* **290**, 41-49 (1993).
3. E. J. Williams, G. L. Hutchinson, F. C. Fehsenfeld, NO_x And N_2O Emissions From Soil. *Global Biogeochemical Cycles* **6**, 351-388 (1992).
4. J. M. Langridge, S. M. Ball, R. L. Jones, A compact broadband cavity enhanced absorption spectrometer for detection of atmospheric NO_2 using light emitting diodes. *Analyst* **131**, 916-922 (2006).
5. C. D. Georgiou, I. Papapostolou, K. Grintzalis, Superoxide radical detection in cells, tissues, organisms (animals, plants, insects, microorganisms) and soils. *Nature Protocols* **3**, 1679-1692 (2008).
6. J. Zielonka, J. Vasquez-Vivar, B. Kalyanaraman, Detection of 2-hydroxyethidium in cellular systems: a unique marker product of superoxide and hydroethidine. *Nature Protocols* **3**, 8-21 (2008).
7. K. M. Robinson, J. S. Beckman, "Synthesis of Peroxynitrite from Nitrite and Hydrogen Peroxide" in Methods in Enzymology. (Academic Press, 2005), vol. 396, pp. 207-214.